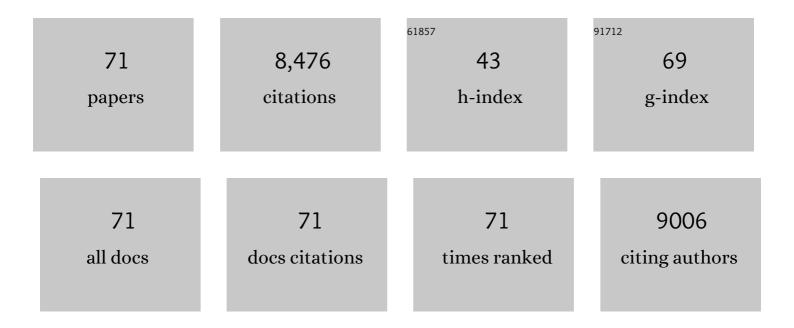
## **Ting Xiong**

List of Publications by Year in descending order

Source: https://exaly.com/author-pdf/11518364/publications.pdf Version: 2024-02-01



TINC YIONC

#	Article	IF	CITATIONS
1	Stretchable <scp>fiberâ€shaped</scp> aqueous aluminum ion batteries. EcoMat, 2022, 4, .	6.8	14
2	Direct ink writing of programmable functional siliconeâ€based composites for 4D printing applications. , 2022, 1, 507-516.		25
3	Pulmonary Targeting Crosslinked Cyclodextrin Metal–Organic Frameworks for Lung Cancer Therapy. Advanced Functional Materials, 2021, 31, 2004550.	7.8	35
4	Unraveling MoS <sub>2</sub> and Transition Metal Dichalcogenides as Functional Zincâ€lon Battery Cathode: A Perspective. Small Methods, 2021, 5, e2000815.	4.6	76
5	Dendrite-Free Anodes Enabled by a Composite of a ZnAl Alloy with a Copper Mesh for High-Performing Aqueous Zinc-Ion Batteries. ACS Applied Materials & Interfaces, 2021, 13, 28129-28139.	4.0	47
6	Harnessing oxygen vacancy in V2O5 as high performing aqueous zinc-ion battery cathode. Journal of Alloys and Compounds, 2021, 870, 159403.	2.8	45
7	Metal Organic framework derived carbon for ultrahigh power and long cyclic life aqueous Zn ion capacitor. Nano Materials Science, 2020, 2, 159-163.	3.9	37
8	3D-Printed Grids with Polymeric Photocatalytic System as Flexible Air Filter. Applied Catalysis B: Environmental, 2020, 262, 118307.	10.8	28
9	Bismuth ion battery – A new member in trivalent battery technology. Energy Storage Materials, 2020, 25, 100-104.	9.5	3
10	New insight into modification of extracellular polymeric substances extracted from waste activated sludge by homogeneous Fe(II)/persulfate process. Chemosphere, 2020, 247, 125804.	4.2	24
11	Bi2S3 for Aqueous Zn Ion Battery with Enhanced Cycle Stability. Nano-Micro Letters, 2020, 12, 8.	14.4	58
12	Energy Harvesting from Atmospheric Humidity by a Hydrogel-Integrated Ferroelectric-Semiconductor System. Joule, 2020, 4, 176-188.	11.7	94
13	Guaranteeing Complete Salt Rejection by Channeling Saline Water through Fluidic Photothermal Structure toward Synergistic Zero Energy Clean Water Production and <i>In Situ</i> Energy Generation. ACS Energy Letters, 2020, 5, 3397-3404.	8.8	129
14	Defect Engineering in Manganeseâ€Based Oxides for Aqueous Rechargeable Zincâ€Ion Batteries: A Review. Advanced Energy Materials, 2020, 10, 2001769.	10.2	249
15	Manipulating unidirectional fluid transportation to drive sustainable solar water extraction and brine-drenching induced energy generation. Energy and Environmental Science, 2020, 13, 4891-4902.	15.6	162
16	Engineering sulphur vacancy in VS <sub>2</sub> as high performing zinc-ion batteries with high cyclic stability. New Journal of Chemistry, 2020, 44, 15951-15957.	1.4	23
17	Oxygenâ€Deficient Birnessiteâ€MnO <sub>2</sub> for Highâ€Performing Rechargeable Aqueous Zinc″on Batteries. ChemNanoMat, 2020, 6, 1357-1364.	1.5	22
18	Preaddition of Cations to Electrolytes for Aqueous 2.2 V High Voltage Hybrid Supercapacitor with Superlong Cycling Life and Its Energy Storage Mechanism. ACS Applied Materials & Interfaces, 2020, 12, 17659-17668.	4.0	27

TING XIONG

#	Article	IF	CITATIONS
19	Structure Architecting for Saltâ€Rejecting Solar Interfacial Desalination to Achieve Highâ€Performance Evaporation With In Situ Energy Generation. Advanced Science, 2020, 7, 1903478.	5.6	224
20	Recent Progress on Fullerene-Based Materials: Synthesis, Properties, Modifications, and Photocatalytic Applications. Materials, 2020, 13, 2924.	1.3	29
21	Mechanistic insights into heavy metals affinity in magnetic MnO2@Fe3O4/poly(m-phenylenediamine) coreâ^'shell adsorbent. Ecotoxicology and Environmental Safety, 2020, 192, 110326.	2.9	29
22	Integrating the (311) facet of MnO2 and the fuctional groups of poly(m-phenylenediamine) in core–shell MnO2@poly(m-phenylenediamine) adsorbent to remove Pb ions from water. Journal of Hazardous Materials, 2020, 389, 122154.	6.5	31
23	Interlayer Engineering of MnO <sub>2</sub> with High Charge Density Bi <sup>3+</sup> for High Rate and Stable Aqueous Supercapacitor. Batteries and Supercaps, 2020, 3, 519-526.	2.4	27
24	Hexagonal MoO <sub>3</sub> as a zinc intercalation anode towards zinc metal-free zinc-ion batteries. Journal of Materials Chemistry A, 2020, 8, 9006-9012.	5.2	91
25	Biochar Facilitated Hydroxyapatite/Calcium Silicate Hydrate for Remediation of Heavy Metals Contaminated Soils. Water, Air, and Soil Pollution, 2020, 231, 1.	1.1	30
26	Efficient incorporation and protection of lansoprazole in cyclodextrin metal-organic frameworks. International Journal of Pharmaceutics, 2020, 585, 119442.	2.6	15
27	Stateâ€ofâ€theâ€Art Advances and Challenges of Ironâ€Based Metal Organic Frameworks from Attractive Features, Synthesis to Multifunctional Applications. Small, 2019, 15, e1803088.	5.2	111
28	A real filed phytoremediation of multi-metals contaminated soils by selected hybrid sweet sorghum with high biomass and high accumulation ability. Chemosphere, 2019, 237, 124536.	4.2	39
29	Defect Engineering of Oxygenâ€Deficient Manganese Oxide to Achieve Highâ€Performing Aqueous Zinc Ion Battery. Advanced Energy Materials, 2019, 9, 1803815.	10.2	504
30	Binder-free V <sub>2</sub> O <sub>5</sub> /CNT paper electrode for high rate performance zinc ion battery. Nanoscale, 2019, 11, 19723-19728.	2.8	68
31	Synergistically Configuring Intrinsic Activity and Fin-Tube-Like Architecture of Mn-Doped MoS <sub>2</sub> -Based Catalyst for Improved Hydrogen Evolution Reaction. ACS Applied Energy Materials, 2019, 2, 493-502.	2.5	40
32	KCl-mediated dual electronic channels in layered g-C <sub>3</sub> N <sub>4</sub> for enhanced visible light photocatalytic NO removal. Nanoscale, 2018, 10, 8066-8074.	2.8	126
33	Insight on the plasmonic Z-scheme mechanism underlying the highly efficient photocatalytic activity of silver molybdate/silver vanadate composite in rhodamine B degradation. Journal of Colloid and Interface Science, 2018, 530, 493-504.	5.0	40
34	In-situ synthesis of direct solid-state dual Z-scheme WO3/g-C3N4/Bi2O3 photocatalyst for the degradation of refractory pollutant. Applied Catalysis B: Environmental, 2018, 227, 376-385.	10.8	495
35	Near-infrared-driven Cr( <scp>vi</scp> ) reduction in aqueous solution based on a MoS <sub>2</sub> /Sb <sub>2</sub> S <sub>3</sub> photocatalyst. Catalysis Science and Technology, 2018, 8, 1545-1554.	2.1	41
36	Harmonizing Energy and Power Density toward 2.7 V Asymmetric Aqueous Supercapacitor. Advanced Energy Materials, 2018, 8, 1702630.	10.2	201

TING XIONG

#	Article	IF	CITATIONS
37	Effect of high intensity ultrasound on structure and foaming properties of pea protein isolate. Food Research International, 2018, 109, 260-267.	2.9	249
38	Implication of graphene oxide in Cd-contaminated soil: A case study of bacterial communities. Journal of Environmental Management, 2018, 205, 99-106.	3.8	75
39	Immobilization of heavy metals in two contaminated soils using a modified magnesium silicate stabilizer. Environmental Science and Pollution Research, 2018, 25, 32562-32571.	2.7	31
40	A facile band alignment of polymeric carbon nitride isotype heterojunctions for enhanced photocatalytic tetracycline degradation. Environmental Science: Nano, 2018, 5, 2604-2617.	2.2	93
41	Modified stannous sulfide nanoparticles with metal-organic framework: Toward efficient and enhanced photocatalytic reduction of chromium (VI) under visible light. Journal of Colloid and Interface Science, 2018, 530, 481-492.	5.0	89
42	Optimizing Electrolyte Physiochemical Properties toward 2.8 V Aqueous Supercapacitor. ACS Applied Energy Materials, 2018, 1, 3070-3076.	2.5	28
43	<i>o</i> â€Benzenediolâ€Functionalized Carbon Nanosheets as Low Selfâ€Discharge Aqueous Supercapacitors. ChemSusChem, 2018, 11, 3307-3314.	3.6	27
44	Visible-light-driven removal of tetracycline antibiotics and reclamation of hydrogen energy from natural water matrices and wastewater by polymeric carbon nitride foam. Water Research, 2018, 144, 215-225.	5.3	481
45	Bi metal sphere/graphene oxide nanohybrids with enhanced direct plasmonic photocatalysis. Applied Catalysis B: Environmental, 2017, 214, 148-157.	10.8	98
46	Activation of amorphous bismuth oxide via plasmonic Bi metal for efficient visible-light photocatalysis. Journal of Catalysis, 2017, 352, 102-112.	3.1	135
47	Mn <sub>3</sub> O <sub>4</sub> /reduced graphene oxide based supercapacitor with ultra-long cycling performance. Journal of Materials Chemistry A, 2017, 5, 12762-12768.	5.2	70
48	Indole-based conjugated macromolecules as a redox-mediated electrolyte for an ultrahigh power supercapacitor. Energy and Environmental Science, 2017, 10, 2441-2449.	15.6	68
49	Highly efficient visible-light-induced photoactivity of Z-scheme Ag <sub>2</sub> CO <sub>3</sub> /Ag/WO <sub>3</sub> photocatalysts for organic pollutant degradation. Environmental Science: Nano, 2017, 4, 2175-2185.	2.2	121
50	Exploring the photocatalysis mechanism on insulators. Applied Catalysis B: Environmental, 2017, 219, 450-458.	10.8	48
51	Single Precursor Mediated-Synthesis of Bi Semimetal Deposited N-Doped (BiO) <sub>2</sub> CO <sub>3</sub> Superstructures for Highly Promoted Photocatalysis. ACS Sustainable Chemistry and Engineering, 2016, 4, 2969-2979.	3.2	64
52	Facets and defects cooperatively promote visible light plasmonic photocatalysis with Bi nanowires@BiOCl nanosheets. Journal of Catalysis, 2016, 344, 401-410.	3.1	172
53	Three dimensional Z-scheme (BiO) 2 CO 3 /MoS 2 with enhanced visible light photocatalytic NO removal. Applied Catalysis B: Environmental, 2016, 199, 87-95.	10.8	133
54	Interlayer-I-doped BiOIO <sub>3</sub> nanoplates with an optimized electronic structure for efficient visible light photocatalysis. Chemical Communications, 2016, 52, 8243-8246.	2.2	66

TING XIONG

#	Article	IF	CITATIONS
55	Bridging the g-C <sub>3</sub> N <sub>4</sub> Interlayers for Enhanced Photocatalysis. ACS Catalysis, 2016, 6, 2462-2472.	5.5	869
56	Ternary Ag/AgCl/BiOIO3 composites for enhanced visible-light-driven photocatalysis. Chinese Journal of Catalysis, 2015, 36, 2155-2163.	6.9	54
57	New insights into how RGO influences the photocatalytic performance of BiOIO3/RGO nanocomposites under visible and UV irradiation. Journal of Colloid and Interface Science, 2015, 447, 16-24.	5.0	71
58	Synergistic integration of thermocatalysis and photocatalysis on black defective (BiO) <sub>2</sub> CO <sub>3</sub> microspheres. Journal of Materials Chemistry A, 2015, 3, 18466-18474.	5.2	67
59	Improving g-C3N4 photocatalysis for NOx removal by Ag nanoparticles decoration. Applied Surface Science, 2015, 358, 356-362.	3.1	101
60	Controlling interfacial contact and exposed facets for enhancing photocatalysis via 2D–2D heterostructures. Chemical Communications, 2015, 51, 8249-8252.	2.2	145
61	In situ synthesis of a C-doped (BiO) <sub>2</sub> CO <sub>3</sub> hierarchical self-assembly effectively promoting visible light photocatalysis. Journal of Materials Chemistry A, 2015, 3, 6118-6127.	5.2	103
62	Growth mechanism and photocatalytic activity of self-organized N-doped (BiO) <sub>2</sub> CO <sub>3</sub> hierarchical nanosheet microspheres from bismuth citrate and urea. Dalton Transactions, 2014, 43, 6631-6642.	1.6	45
63	Growth of BiOBr nanosheets on C3N4 nanosheets to construct two-dimensional nanojunctions with enhanced photoreactivity for NO removal. Journal of Colloid and Interface Science, 2014, 418, 317-323.	5.0	136
64	Enhanced extrinsic absorption promotes the visible light photocatalytic activity of wide band-gap (BiO) <sub>2</sub> CO <sub>3</sub> hierarchical structure. RSC Advances, 2014, 4, 56307-56312.	1.7	47
65	The rapid synthesis of photocatalytic (BiO) <sub>2</sub> CO <sub>3</sub> single-crystal nanosheets via an eco-friendly approach. CrystEngComm, 2014, 16, 3592-3604.	1.3	25
66	A semimetal bismuth element as a direct plasmonic photocatalyst. Chemical Communications, 2014, 50, 10386-10389.	2.2	282
67	Effects of Morphology and Crystallinity on the Photocatalytic Activity of (BiO) <sub>2</sub> CO <sub>3</sub> Nano/microstructures. Industrial & Engineering Chemistry Research, 2014, 53, 15002-15011.	1.8	66
68	Synthesis of BiOBr–graphene and BiOBr–graphene oxide nanocomposites with enhanced visible light photocatalytic performance. Ceramics International, 2014, 40, 9003-9008.	2.3	40
69	In Situ Construction of g-C <sub>3</sub> N <sub>4</sub> /g-C <sub>3</sub> N <sub>4</sub> Metal-Free Heterojunction for Enhanced Visible-Light Photocatalysis. ACS Applied Materials & Interfaces, 2013, 5, 11392-11401.	4.0	1,102
70	Ammonia induced formation of N-doped (BiO)2CO3 hierarchical microspheres: the effect of hydrothermal temperature on the morphology and photocatalytic activity. CrystEngComm, 2013, 15, 10522.	1.3	26
71	K <sup>+</sup> -Intercalated MnO <sub>2</sub> Electrode for High Performance Aqueous Supercapacitor. ACS Applied Energy Materials, 0, , .	2.5	10